Journal of Nonlinear Modeling and Analysis
Volume 3, Number 2, June 2021, 193–207
http://jnma.ca; http://jnma.ijournal.cn
DOI:10.12150/jnma.2021.193

Bifurcations and New Traveling Wave Solutions for the Nonlinear Dispersion Drinfel'd-Sokolov ($D(m,n)$) System*

Ronghua Cheng[1,2], Zhaofu Luo[2] and Xiaochun Hong[2,†]

Abstract In this paper, we employ the theory of the planar dynamical system to investigate the dynamical behavior and bifurcations of solutions of the traveling systems of the $D(m,n)$ equation. On the basis of the previous work of the reference [17], we obtain the solitary cusp waves solutions (peakons and valleyons), breaking wave solutions (compactons) and other periodic cusp wave solutions. Morever, we make a summary of exact traveling wave solutions to the $D(m,n)$ system including all the solutions which have been found from the references [4, 14, 17].

Keywords $D(m,n)$ system, Solitary wave solution, Periodic wave solution, Compacton, Peakon.

MSC(2010) 35B10, 35C07, 35C08.

1. Introduction

In this paper, we consider the following nonlinear dispersion Drinfel'd-Sokolov system ($D(m,n)$ system)

$$q_t + k(r^m)_x = 0, \tag{1.1a}$$
$$r_t + a(r^n)_{xxx} + bq_xr + cqr_x = 0, \tag{1.1b}$$

where m, n are positive integer, a, b, c, k are real valued constants. The physical application of this model can be seen in references [6, 7] and the references therein.

For the coupled system, Biswas et al. [1] and Chen et al. [3] obtained the three kinds of solutions when (m,n)=(1,1) by using the method of exponential function and dynamical systems method respectively. In 2011, Ebadi et al. [5] obtained one-soliton solution of the $D(m,n)$ equation by the ansatz method. Xie et al. [14] have obtained the compact and solitary patterns solutions of the $D(m,n)$ equation by using the sine-cosine method and the sinh-cosh method. Deng et al. [4] have studied some particular travelling wave solutions of the $D(m,n)$ equation by using the Weierstrass elliptic function expansion method. Zhang et al. [17] have obtained

†the corresponding author.
Email address: ronghua_cheng@yeah.net(R. Cheng), zhaofu_luo@yeah.net(Z. Luo), xchong@ynufe.edu.cn(X. Hong)
1School of Mathematics and Statistics, Nanjing University of Information Science and Technology, Nanjing, Jiangsu 210044, China
2School of Statistics and Mathematics, Yunnan University of Finance and Economics, Kunming, Yunnan 650221, China
*The authors were supported by National Natural Science Foundation of China (No. 11761075).

some travelling wave solutions by using the bifurcation theory of planar dynamical systems.

Though many authors have studied the $D(m,n)$ system, they only obtained relatively partial exact solutions. The paper will be further to study the issue on the basis of the previous work. We make some complement, expansion and summary to the solutions of the coupled system (1.1). Moreover, by using the bifurcation method of planar systems and simulation method of differential equations ([8–13, 15, 16]), we shall study the exact explicit bounded travelling wave solutions of (1.1) under different parameter condition.

2. Transformed equations

Using the traveling wave assumption that

$$q(x,t) = \phi(\xi), \tag{2.1a}$$
$$r(x,t) = \psi(\xi), \tag{2.1b}$$

where $\xi = x - \lambda t$ is the real parameter and λ is the wave speed, substituting (2.1) into Equations.(1.1), we can reduce Equations (1.1) to the following ODEs:

$$-\lambda\phi' + k(\psi^m)' = 0, \tag{2.2a}$$
$$-\lambda\psi' + a(\psi^n)''' + b\phi'\psi + c\phi\psi' = 0. \tag{2.2b}$$

Integrating (2.2a) once and letting integral constant to be zero, we have

$$\phi = \frac{k}{\lambda}\psi^m. \tag{2.3}$$

Inserting (2.3) to Equation (2.2b) yields

$$-\lambda\psi' + a(\psi^n)''' + \frac{k}{\lambda}(bm + c)\psi^m\psi' = 0. \tag{2.4}$$

Integrating (2.4) once, we obtain

$$\frac{\lambda}{a}\psi - n(n-1)(\psi^{n-2})\psi'^2 - n\psi^{n-1}\psi'' - \frac{k(bm+c)}{a\lambda(m+1)}\psi^{m+1} + A = 0, \tag{2.5}$$

which is equivalent to 2-dimensional Hamiltonian system

$$\frac{d\psi}{d\xi} = y, \quad \frac{dy}{d\xi} = \frac{-n(n-1)\psi^{n-2}y^2 + \alpha\psi - \frac{\beta(bm+c)}{m+1}\psi^{m+1} + A}{n\psi^{n-1}}, \tag{2.6}$$

where A is a integrating constant and $\alpha = \frac{\lambda}{a}$, $\beta = \frac{k}{a\lambda}$ with the first integral

$$H(\psi, y) = \frac{n}{2}\psi^{2(n-1)}y^2 - \frac{A}{n}\psi^n - \frac{\alpha}{n+1}\psi^{n+1} + \frac{\beta(bm+c)}{(m+1)(m+n+1)}\psi^{m+n+1} = h. \tag{2.7}$$

3. Bifurcations of phase portraits of the traveling system

Letting $d\eta = an\psi^{n-1}d\xi$, the system (2.6) becomes the following regular system

$$\frac{d\psi}{d\eta} = n\psi^{n-1}y, \quad \frac{dy}{d\eta} = -n(n-1)\psi^{n-2}y^2 + \alpha\psi - \frac{\beta(bm+c)}{m+1}\psi^{m+1} + A, \quad (3.1)$$

which has the same invariant curves as system (2.6) except for the straight line $\psi = 0$. Take that

$$f(\psi) = A + \alpha\psi - \frac{\beta(bm+c)}{m+1}\psi^{m+1}.$$

Let $M(\psi_i,\ y_j)$ be the coefficient matrix of the linearized system of (3.1) at an equilibrium point (ψ_i, y_j), we have

$$J(\psi_i, y_j) = -n^3(n-1)\psi_i^{2(n-2)}y_j^2 - n\psi^{n-1}f'(\psi_i). \quad (3.2)$$

3.1. The case of $A = 0$

When $A = 0$, write that $f_0(\psi) = \alpha\psi - \frac{\beta(bm+c)}{m+1}\psi^{m+1}$. On the (ψ, y)-phase plane, the abscissas of equilibrium points of the system (3.1) on the ψ-axis are the zeros of $f_0(\psi)$. Clearly, when m is an even integer and $\alpha\beta(bm+c) < 0$, it means that system (3.1) has only one equilibrium point at $O(0,0)$; when m is an even integer and $\alpha\beta(bm+c) > 0$, the system (3.1) has three equilibrium points at $O(0,0)$, $E_1(\psi_1, 0)$ and $E_2(\psi_2, 0)$, where $\psi_{1,2} = \pm\sqrt[m]{\frac{\alpha(m+1)}{\beta(bm+c)}}$. When m is an odd integer, the system (3.1) has two equilibrium points at $O(0,0)$ and $E_1(\psi_1, 0)$.

Thus, we know system (3.1) has at most three equilibrium points in the ψ-axis. Writing that

$$J_0(\psi_i, 0) = -n\psi_i^{n-1}\left[\alpha - \beta(bm+c)\psi_i^m\right].$$

By the qualitative theory of dynamical systems, we can determine that an equilibrium point is a center or saddle point. Write that

$$h_0 = H(0,0) = 0, \quad h_1 = h_2 = H(\psi_{1,2}, 0) = \frac{-\alpha m}{(n+1)(m+n+1)}\left[\frac{\alpha(m+1)}{\beta(bm+c)}\right]^{\frac{n+1}{m}},$$

where H is defined by (2.7).

By using the above information, under different parameter conditions, we obtain the following phase portraits for system (3.1) shown in Figures 1–5.

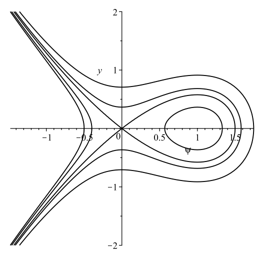

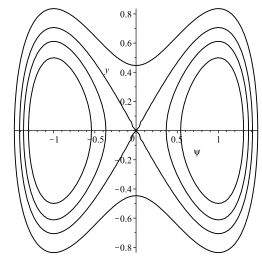

(a) $m = 2K - 1,\ \alpha > 0,\ \beta(mb + c) > 0$ (b) $m = 2K,\ \alpha > 0,\ \beta(mb + c) > 0$

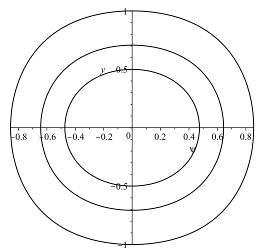

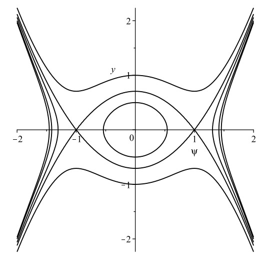

(c) $m = 2K,\ \alpha < 0,\ \beta(mb + c) > 0$ (d) $m = 2K,\ \alpha < 0,\ \beta(mb + c) < 0$

Figure 1. The bifurcation phase portraits of the system (3.1) for $n = 1,\ A = 0,\ K = 1, 2, \cdots$

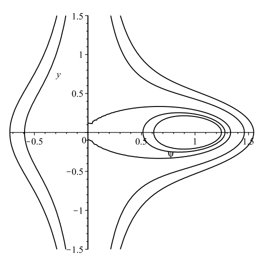

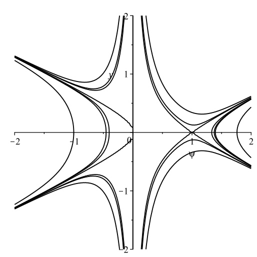

(a) $m = 2K - 1, \alpha > 0, \beta(mb + c) > 0$ (b) $m = 2K - 1, \alpha < 0, \beta(mb + c) < 0$

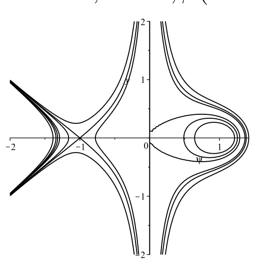

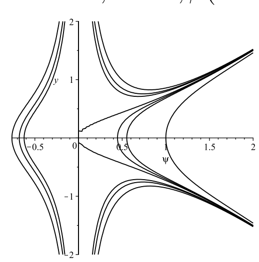

(c) $m = 2K, \alpha > 0, \beta(mb + c) > 0$ (d) $m = 2K, \alpha > 0, \beta(mb + c) < 0$

Figure 2. The bifurcation phase portraits of the system (3.1) for $n = 2, A = 0,\ K = 1, 2, \cdots$

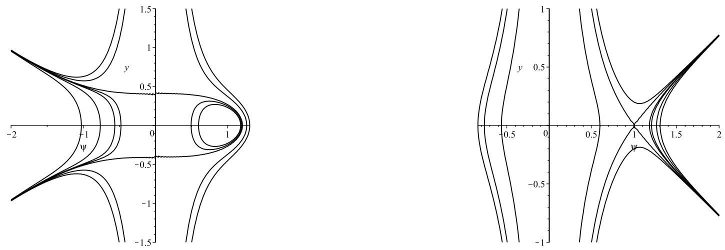

(a) $m = 2K-1, \alpha > 0, \beta(mb+c) > 0$ (b) $m = 2K-1, \alpha < 0, \beta(mb+c) < 0$

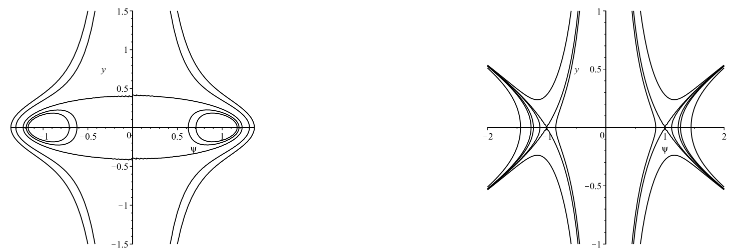

(c) $m = 2K, \alpha > 0, \beta(mb+c) > 0$ (d) $m = 2K, \alpha < 0, \beta(mb+c) < 0$

Figure 3. The bifurcation phase portraits of the system (3.1) for $n = 3, A = 0,\ K = 1, 2, \cdots$

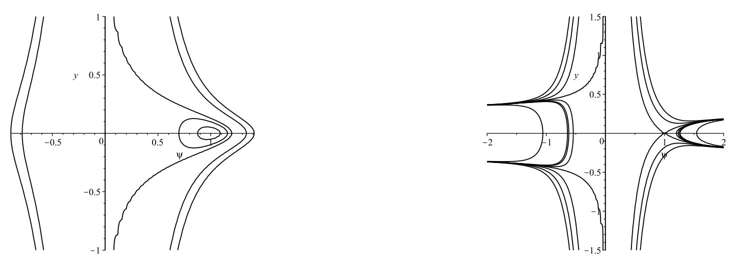

(a) $m = 2K-1, \alpha > 0, \beta(mb+c) > 0$ (b) $m = 2K-1, \alpha < 0, \beta(mb+c) < 0$

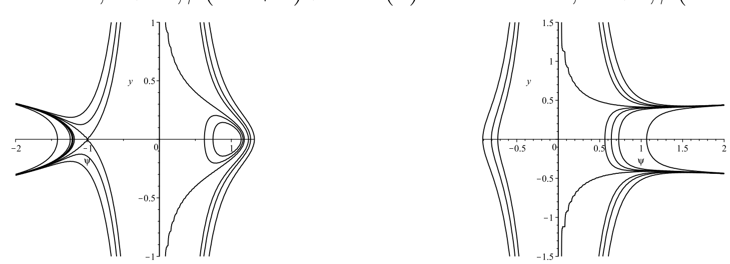

(c) $m = 2K, \alpha > 0, \beta(mb+c) > 0$ (d) $m = 2K, \alpha > 0, \beta(mb+c) < 0$

Figure 4. The bifurcation phase portraits of the system (3.1) for $n = 2L, L = 2, 3, \cdots, A = 0,$ $K = 1, 2, \cdots$

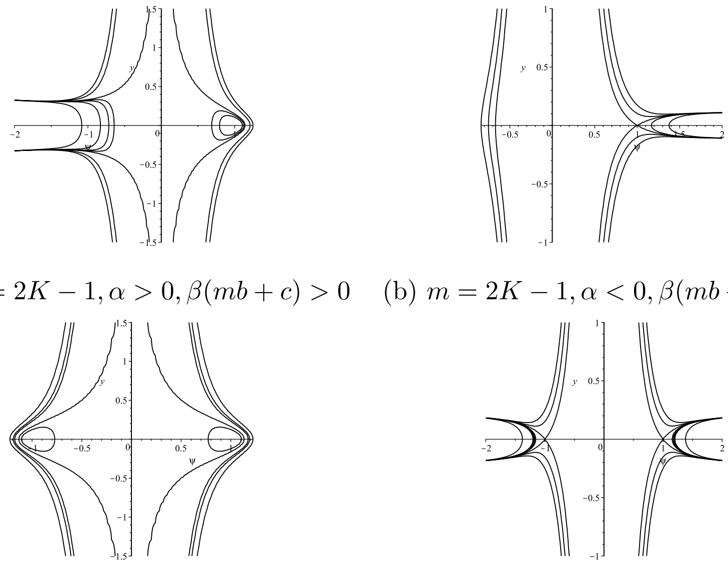

(a) $m = 2K - 1, \alpha > 0, \beta(mb + c) > 0$ (b) $m = 2K - 1, \alpha < 0, \beta(mb + c) < 0$

(c) $m = 2K, \alpha > 0, \beta(mb + c) > 0$ (d) $m = 2K, \alpha < 0, \beta(mb + c) < 0$

Figure 5. The bifurcation phase portraits of the system (3.1) for $n = 2L + 1, L = 2, 3, \cdots, A = 0$, $K = 1, 2, \cdots$

3.2. The case of $A \neq 0$

In this case, we consider that there exist equilibrium points on y-axis. When $n = 2$, $A > 0$, there are two equilibrium points of (3.1) at $F_1(0, -\sqrt{\frac{A}{2}})$ and $F_2(0, \sqrt{\frac{A}{2}})$ on y-axis . Whereas when $n > 2$, system (3.1) has no equilibrium point on y-axis if $A \neq 0$.

Notice that $f'(\psi) = \alpha - \beta(bm + c)\psi^m$, $f''(\psi) = -\beta m(bm + c)\psi^{m-1}$ and $f(0) = A(> 0)$. Obviously, when m is an odd integer, $f'(\psi)$ has one zero point $\widetilde{\psi} = \sqrt[m]{\frac{\alpha}{\beta(bm+c)}}$, $f(\psi)$ has two zeros ψ_i for $i = 1, 2$. Thus, system (3.1) has two equilibrium points on the ψ-axis. When m is an even integer, $f'(\psi)$ has two zeros points $\psi_\pm = \pm\sqrt[m]{\frac{\alpha}{\beta(bm+c)}}$ if $\alpha\beta(bm + c) > 0$, $f(\psi)$ has at most three zeros ψ_i for $i = 1, 2, 3$. Thus, system (3.1) has at most three equilibrium points on the ψ-axis.

It is clear that two equilibrium points on y-axis are saddle points for $n = 2$. As to the equilibrium points on the ψ-axis, it is a center or a saddle point if $-n\psi^{n-1}f'(\psi) > 0$ or $-n\psi^{n-1}f'(\psi) < 0$. Write that $h_F = H(0, \pm\sqrt{\frac{A}{2}}) = 0$. By using the above information, we obtain some phase portraits in case of $n = 1, 2$ for system (3.1) shown in Figures 6–8.

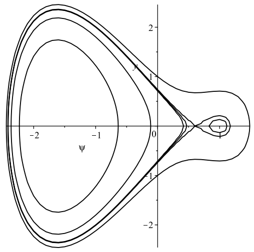
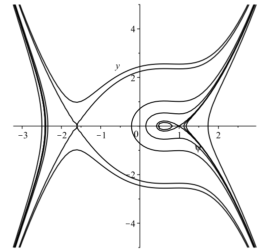

(a) $m = 2K, \alpha > 0, \beta(mb + c) > 0$ (b) $m = 2K, \alpha < 0, \beta(mb + c) < 0$

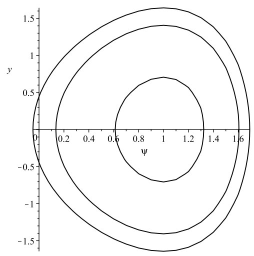
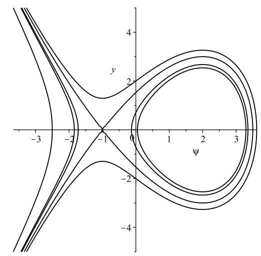

(c) $m = 2K, \alpha < 0, \beta(mb + c) > 0$ (d) $m = 2K - 1, \alpha > 0, \beta(mb + c) > 0$

Figure 6. The bifurcation phase portraits of the system (3.1) for $n = 1, A \neq 0,\ K = 1, 2, \cdots$

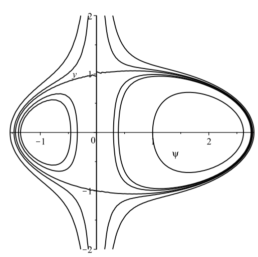
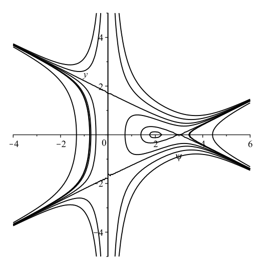

(a) $\psi_1 < 0 < \psi_2$ (b) $0 < \psi_1 < \psi_2, h_2 < h_F$

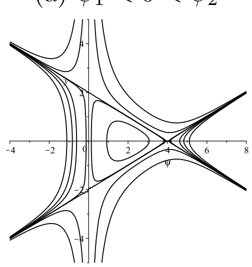
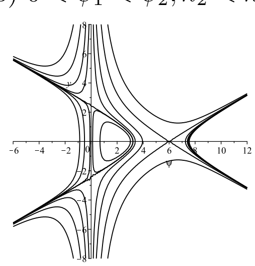

(c) $0 < \psi_1 < \psi_2, h_2 = h_F$ (d) $0 < \psi_1 < \psi_2, h_2 > h_F$

Figure 7. The bifurcation phase portraits of the system (3.1) for $m = 1, n = 2, A > 0$.

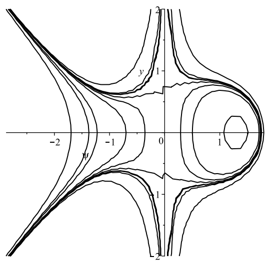

(a) $f(\psi_-) > 0$.

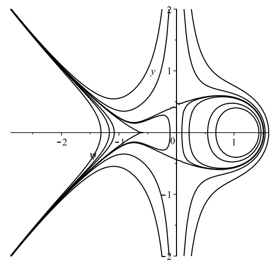

(b) $f(\psi_-) = 0$

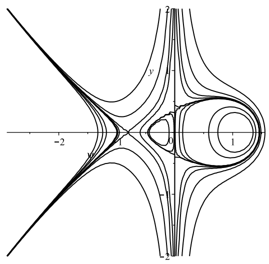

(c) $f(\psi_-) < 0$.

Figure 8. The bifurcation phase portraits of the system (3.1) for $m = 2, n = 2, A > 0,\ \alpha > 0, \beta(mb + c) > 0$.

4. Exact traveling wave solutions of the system (3.1) without the singular straight line $\psi = 0$

For $n = 1$, system (3.1) reduces a non-singular system

$$\frac{d\psi}{d\xi} = y, \quad \frac{dy}{d\xi} = A + \alpha\psi - \frac{\beta(bm + c)}{m+1}\psi^{m+1}. \tag{4.1}$$

The orbits of system (4.1) can be shown in Figure 1 if $A = 0$.

4.1. Infinitely many smooth periodic wave solutions

When $m = 1, \alpha > 0, \beta(b+c) > 0$, see Fig. 1(a), system (4.1) has a periodic solution corresponds to a family of periodic orbits if $h \in (h_1, h_0)$.

$$r(x,t) = \psi(x - ct) = z_3 - (z_3 - z_2)\mathrm{sn}^2\left(\omega_1(x - ct), k_1\right), \tag{4.2a}$$

$$q(x,t) = \phi(x - ct) = a\beta\left[z_3 - (z_3 - z_2)\mathrm{sn}^2\left(\omega_1(x - ct), k_1\right)\right], \tag{4.2b}$$

where z_1, z_2 and z_3 satisfy $z_1 < z_2 < z_3, \omega_1 = \sqrt{\frac{\beta(b+c)(z_3-z_1)}{12}}, k_1 = \sqrt{\frac{z_3-z_2}{z_3-z_1}}$. Similarly, system (4.1) has a periodic solutions corresponding to a family of periodic orbits in Figure 6(d), which has the same parametric representations as (4.2).

When $m = 2$,

(i) $\alpha>0, \beta(b+c)>0$, see Figure 1(b), when $h\in(h_1,h_0)$, system (4.1) has two periodic solutions corresponds to two family of periodic orbits ([3,4]).

$$r(x,t)=\psi(x-ct)=\pm z_5 \mathrm{dn}\left(\sqrt{\frac{\beta(2b+c)}{6}}z_5(x-ct), \frac{\sqrt{z_5^2-z_4^2}}{z_5^2}\right), \tag{4.3a}$$

$$q(x,t)=\phi(x-ct)=a\beta z_5^2 \mathrm{dn}^2\left(\sqrt{\frac{\beta(2b+c)}{6}}z_5(x-ct), \frac{\sqrt{z_5^2-z_4^2}}{z_5^2}\right), \tag{4.3b}$$

where z_4 and z_5 satisfy $z_4^2<z_5^2$.

When $h\in(h_0,\infty)$, system (4.1) has a periodic solutions corresponding to a family of periodic orbits ([4,17]).

$$r(x,t)=\psi(x-ct)=z_7 \mathrm{cn}\left(\sqrt{\frac{\beta(2b+c)(z_6^2+z_7^2)}{6}}(x-ct), \sqrt{\frac{z_7^2}{z_6^2+z_7^2}}\right), \tag{4.4a}$$

$$q(x,t)=\phi(x-ct)=a\beta z_7^2 \mathrm{cn}^2\left(\sqrt{\frac{\beta(2b+c)(z_6^2+z_7^2)}{6}}(x-ct), \sqrt{\frac{z_7^2}{z_6^2+z_7^2}}\right), \tag{4.4b}$$

where z_6 and z_7 satisfy $z_6^2<z_7^2$.

(ii) $\alpha<0, \beta(b+c)>0$, see Figure 1(c), when $h\in(h_0,\infty)$, system (4.1) has a periodic solutions corresponding to a family of periodic orbits, which has the same parametric representations as (4.4).

(iii) $\alpha<0, \beta(b+c)<0$, see Figure 1(d), when $h\in(h_0,h_1)$ $(h_1=h_2)$, system (4.1) has a periodic solutions corresponds to a family of periodic orbits ([3,4,17]).

$$r(x,t)=\psi(x-ct)=z_8 \mathrm{sn}\left(\sqrt{\frac{\lambda\alpha}{2(c-1)}}z_9(x-ct), \frac{z_8}{z_9}\right), \tag{4.5a}$$

$$q(x,t)=\phi(x-ct)=a\beta z_8 \mathrm{sn}\left(\sqrt{\frac{\lambda\alpha}{2(c-1)}}z_9(x-ct), \frac{z_8}{z_9}\right), \tag{4.5b}$$

where z_8 and z_9 satisfy $z_8^2<z_9^2$.

Morever, there exist periodic solutions in Figures 6(a), 6(b), 6(c).

4.2. Infinitely many solitary wave solutions

When $m=1, \alpha>0, \beta(b+c)>0$, see Figure 1(a), system (4.1) has a solitary wave solution corresponding to a homoclinic orbit defined by $h=h_0$ ([3,4]).

$$r(x,t)=\psi(x-ct)=\frac{3\alpha}{\beta(b+c)}\mathrm{sech}^2\left(\frac{1}{2}\sqrt{\alpha}(x-ct)\right), \tag{4.6a}$$

$$q(x,t)=\phi(x-ct)=\frac{3a\alpha}{b+c}\mathrm{sech}^2\left(\frac{1}{2}\sqrt{\alpha}(x-ct)\right). \tag{4.6b}$$

When $m=2$,

(i) $\alpha>0$, $\beta(b+c)>0$, see Figure 1(b), system (4.1) has two solitary wave solutions corresponding to two homoclinic orbit defined by $h=h_0$ ([3,4]).

$$r(x,t)=\psi(x-ct)=\pm\sqrt{\frac{6\alpha}{\beta(2b+c)}}\mathrm{sech}\left(\sqrt{\alpha}(x-ct)\right), \tag{4.7a}$$

$$q(x,t) = \phi(x-ct) = \frac{6a\alpha}{2b+c}\mathrm{sech}^2\left(\sqrt{\alpha}(x-ct)\right). \tag{4.7b}$$

(ii) $\alpha < 0$, $\beta(b+c) < 0$, see Figure 1(d), system (4.1) has kink and anti-kink wave solutions corresponding to two heteroclinic orbits defined by $h = h_1$ ([3,4]).

$$r(x,t) = \psi(x-ct) = \pm\sqrt{\frac{3\alpha}{\beta(2b+c)}}\tanh\left(\sqrt{-\frac{\alpha}{2}}(x-ct)\right), \tag{4.8a}$$

$$q(x,t) = \phi(x-ct) = \frac{3a\alpha}{b+c}\tanh^2\left(\sqrt{-\frac{\alpha}{2}}(x-ct)\right). \tag{4.8b}$$

Morever, there exist solitary wave solutions in Figures 6(a), 6(b), 6(d).

5. Exact explicit parametric representations of traveling wave solutions for the singular system (3.1)

From (2.7), we obtain

$$y^2 = \frac{2}{n\psi^{n-3}}\left[\frac{A}{n\psi} + \frac{\alpha}{n+1} - \frac{\beta(bm+c)}{(m+1)(m+n+1)}\psi^m\right]. \tag{5.1}$$

5.1. Smooth periodic solutions

When $n > 1, A = 0$, the families of periodic orbits of system (3.1) defined by $H(\psi, y) = 0$ can be shown in Figures 2(a), 2(c).

When $m = 1$ (or $m = 2$), $n = 2, \alpha > 0, \beta(b+c) > 0$, we have a periodic solution which corresponds to a compact oval orbit defined by $H(\psi, y) = 0$ ([4,14,17]).

$$D(1,2): \quad r(x,t) = \psi(x-ct) = \frac{8\alpha}{3\beta(b+c)}\cos^2\left(\frac{1}{4}\sqrt{\frac{\beta(b+c)}{2}}(x-ct)\right), \tag{5.2a}$$

$$D(1,2): \quad q(x,t) = \phi(x-ct) = \frac{8a\alpha}{3(b+c)}\cos^2\left(\frac{1}{4}\sqrt{\frac{\beta(b+c)}{2}}(x-ct)\right). \tag{5.2b}$$

The above solutions (5.2) are called "compacton solutions" by F. Xie and Z. Yan ([14]).

$$D(2,2): \quad r(x,t) = \psi(x-ct) = \frac{v_1 \mathrm{sn}^2\left(\sqrt{\frac{u_1 v_1}{2}}(x-ct), \frac{\sqrt{2}}{2}\right)}{2 - \mathrm{sn}^2\left(\sqrt{\frac{u_1 v_1}{2}}(x-ct), \frac{\sqrt{2}}{2}\right)}, \tag{5.3a}$$

$$D(2,2): \quad q(x,t) = \phi(x-ct) = a\beta\left[\frac{v_1 \mathrm{sn}^2\left(\sqrt{\frac{u_1 v_1}{2}}(x-ct), \frac{\sqrt{2}}{2}\right)}{2 - \mathrm{sn}^2\left(\sqrt{\frac{u_1 v_1}{2}}(x-ct), \frac{\sqrt{2}}{2}\right)}\right]^2, \tag{5.3b}$$

where $u_1 = \frac{\beta(2b+c)}{15}, v_1 = \sqrt{\frac{5\alpha}{\beta(2b+c)}}$.

5.2. Periodic cusp wave solutions

When $m = 1$ (or $m = 3$), $n = 3, A = 0, \alpha > 0, \beta(2b + c) > 0$, see Figure 3(a), the boundary curves of the periodic annulus corresponds to the periodic cusp wave solution defined by $H(\psi, y) = 0$.

$$D(1,3): \quad r(x,t) = \psi(x-ct) = \frac{5\alpha}{2\beta(b+c)} - \frac{\beta(b+c)}{60}(x-ct)^2, \tag{5.4a}$$

$$D(1,3): \quad q(x,t) = \phi(x-ct) = \frac{5a\alpha}{2(b+c)} - \frac{a\beta^2(b+c)}{60}(x-ct)^2, \tag{5.4b}$$

where $(x-ct) \in \left[-\frac{5\sqrt{6\alpha}}{\beta(b+c)}, \frac{5\sqrt{6\alpha}}{\beta(b+c)}\right]$.

$$D(3,3): r(x,t) = \psi(x-ct) = u_2 \frac{(\sqrt{3}+1)\mathrm{cn}(\omega_2(x-ct), k_2) - (\sqrt{3}-1)}{\mathrm{cn}\,(\omega_2(x-ct), k_2) + 1}, \tag{5.5a}$$

$$D(3,3): q(x,t) = \phi(x-ct) = a\beta\psi^3(x-ct), \tag{5.5b}$$

where $u_2 = \sqrt[3]{\frac{7\alpha}{\beta(3b+c)}}, \omega_2 = \frac{\alpha^{\frac{1}{6}}[\beta(3b+c)]^{\frac{1}{3}}}{7^{\frac{1}{3}}12^{\frac{1}{4}}}, k_2 = \frac{\sqrt{3}+1}{2\sqrt{2}}$.

When $m = 2, n = 3, A = 0, \alpha > 0, \beta(2b + c) > 0$, see Figure 3(c), the boundary curves of two periodic annulus corresponds to two periodic cusp wave solution defined by $H(\psi, y) = 0$ ([14,17]).

$$r(x,t) = \psi(x-ct) = \pm\frac{3}{2}\sqrt{\frac{2\alpha}{\beta(2b+c)}}\cos\left(\frac{1}{6}\sqrt{\frac{\beta(2b+c)}{3}}(x-ct)\right), \tag{5.6a}$$

$$q(x,t) = \phi(x-ct) = \frac{9a\alpha}{2(2b+c)}\cos^2\left(\frac{1}{6}\sqrt{\frac{\beta(2b+c)}{3}}(x-ct)\right). \tag{5.6b}$$

The above solutions (5.6a) are called "compacton solutions" by F. Xie and Z. Yan ([14]).

When $m = 1, n = 2, A > 0, \alpha > 0, \beta(b + c) > 0$, see Figure 7(a), the boundary curves of two periodic annulus corresponds to two periodic cusp wave solution defined by $H(\psi, y) = 0$.

$$r(x,t) = \psi(x-ct) = \pm\frac{4\alpha}{3\beta(b+c)}\left[1 + \frac{\sqrt{\triangle}}{2}\sin\left(\sqrt{\frac{\beta(b+c)}{8}}(x-ct)\right)\right], \tag{5.7a}$$

$$q(x,t) = \phi(x-ct) = \pm\frac{4a\alpha}{3(b+c)}\left[1 + \frac{\sqrt{\triangle}}{2}\sin\left(\sqrt{\frac{\beta(b+c)}{8}}(x-ct)\right)\right], \tag{5.7b}$$

where $\triangle = 4\alpha^2 + 9A\beta(b + c)$.

Moreover, there exist periodic cusp wave solutions in Figures 7(a), 8(a), 8(b).

5.3. Breaking wave solutions (compactons)

When $m = n - 1, n > 3, \alpha > 0, \beta(bm + c) > 0$, see Figures 4(a) and 5(c), we have breaking wave solutions (compactons) defined by $H(\psi, y) = 0$.

(A) For $m = 2K - 1$,

$$r(x,t) = \psi(x - ct) = \left[\frac{2\alpha(m+1)^2}{\beta(bm+c)(m+2)}\cos^2\left(\frac{1}{2}\sqrt{\frac{\beta(bm+c)}{(m+1)^3}}(x-ct)\right)\right]^{\frac{1}{m}}, \tag{5.8a}$$

$$q(x,t) = \phi(x - ct) = \frac{2a\alpha(m+1)^2}{(bm+c)(m+2)}\cos^2\left(\frac{1}{2}\sqrt{\frac{\beta(bm+c)}{(m+1)^3}}(x-ct)\right), \tag{5.8b}$$

where $(x-ct) \in \left[-\sqrt{\frac{(m+1)^3}{\beta(bm+c)}}\pi, \sqrt{\frac{(m+1)^3}{\beta(bm+c)}}\pi\right)$, which corresponds to one open orbit.

(B) $m = 2K$,

$$r(x,t) = \psi(x - ct) = \pm\left[\frac{2\alpha(m+1)^2}{\beta(bm+c)(m+2)}\cos^2\left(\frac{1}{2}\sqrt{\frac{\beta(bm+c)}{(m+1)^3}}(x-ct)\right)\right]^{\frac{1}{m}}, \tag{5.9a}$$

$$q(x,t) = \phi(x - ct) = \frac{2a\alpha(m+1)^2}{(bm+c)(m+2)}\cos^2\left(\frac{1}{2}\sqrt{\frac{\beta(bm+c)}{(m+1)^3}}(x-ct)\right), \tag{5.9b}$$

where $(x-ct) \in \left[-\sqrt{\frac{(m+1)^3}{\beta(bm+c)}}\pi, \sqrt{\frac{(m+1)^3}{\beta(bm+c)}}\pi\right)$, which corresponds to two open orbits.

Moreover, there exist breaking wave solutions (compactons) in Figures 4(c), 4(d), 5(a).

5.4. Solitary cusp waves solutions (peakons and valleyons)

For $m = 1, n = 2, \alpha < 0, \beta(bm + c) < 0$, the curve triangle in Figure 7(c) defined $H(\psi, y) = h_s$ are $y = \mp\sqrt{\frac{|\beta|(b+c)}{8}}\left(\frac{4\alpha}{3\beta(b+c)} - \psi\right)$, which give rise to a solitary cusp (valleyon) wave solution

$$r(x,t) = \psi(x - ct) = \frac{4\alpha}{3\beta(b+c)} - \exp\left(-\sqrt{\frac{|\beta|(b+c)}{8}}|x-ct|\right), \tag{5.10a}$$

$$q(x,t) = \phi(x - ct) = \frac{4a\alpha}{3(b+c)} - a\beta\exp\left(-\sqrt{\frac{|\beta|(b+c)}{8}}|x-ct|\right). \tag{5.10b}$$

For $m = 1, n = 2, \alpha > 0, \beta(bm + c) < 0$, we obtain a solitary cusp (peakon) wave solution again

$$r(x,t) = \psi(x - ct) = \frac{4\alpha}{3\beta(b+c)} + \exp\left(-\sqrt{\frac{|\beta|(b+c)}{8}}|x-ct|\right), \tag{5.11a}$$

$$q(x,t) = \phi(x - ct) = \frac{4a\alpha}{3(b+c)} + a\beta\exp\left(-\sqrt{\frac{|\beta|(b+c)}{8}}|x-ct|\right). \tag{5.11b}$$

Figure 9 below shows solitary cusp of two types.

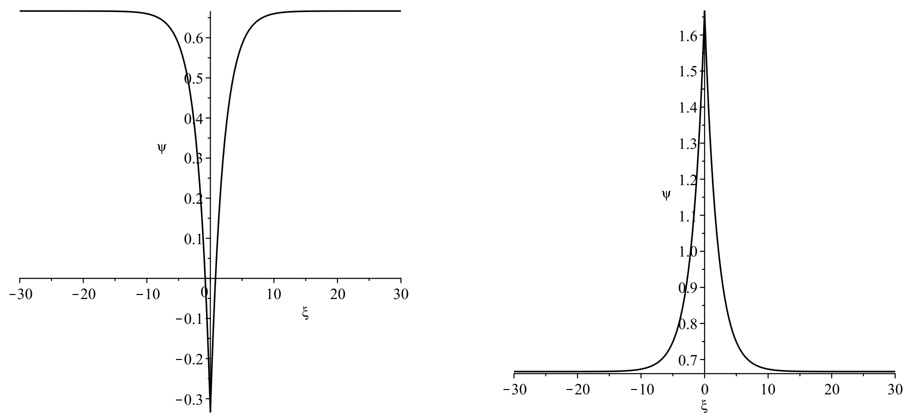

(a) $\alpha < 0,\ \beta(mb+c) < 0$ (b) $\alpha > 0,\ \beta(mb+c) < 0$

Figure 9. The solitary cusp waves $r(x,t)$ of two types (valleyons and peakons) for the system (3.1) when $m = 1,\ n = 2,\ A > 0$.

5.5. Other type of the traveling waves solutions

When $m = n-1$, $n = 2K$, $\alpha < 0$, $\beta(bm+c) < 0$, we have two unbounded traveling wave solutions defined by $H(\psi, y) = 0$ corresponding to two open orbits passsing through $(0,0)$ and $(\psi_1, 0)$ in Figures 2(b) and 4(b).

$$r(x,t) = \psi(x-ct) = \left[\frac{2\alpha(m+1)^2}{\beta(bm+c)(m+2)}\cosh^2\left(\frac{1}{2}\sqrt{\frac{|\beta(bm+c)|}{(m+1)^3}}(x-ct)\right)\right]^{\frac{1}{m}}, \tag{5.12a}$$

$$q(x,t) = \phi(x-ct) = \frac{2a|\alpha|(m+1)^2}{(bm+c)(m+2)}\cosh^2\left(\frac{1}{2}\sqrt{\frac{|\beta(bm+c)|}{(m+1)^3}}(x-ct)\right). \tag{5.12b}$$

When $m = n-1$, $n = 2K+1$, $\alpha < 0$, $\beta(bm+c) < 0$, we have an unbounded traveling wave solutions defined by $H(\psi, y) = 0$ corresponding to the open orbit passsing through $(\psi_1, 0)$ and $(\psi_2, 0)$ in Figures 3(d) and 5(d).

$$r(x,t) = \psi(x-ct) = \left[\frac{2\alpha(m+1)^2}{\beta(bm+c)(m+2)}\cosh^2\left(\frac{1}{2}\sqrt{\frac{|\beta(bm+c)|}{(m+1)^3}}(x-ct)\right)\right]^{\frac{1}{m}}, \tag{5.13a}$$

$$q(x,t) = \phi(x-ct) = \frac{2a\alpha(m+1)^2}{(bm+c)(m+2)}\cosh^2\left(\frac{1}{2}\sqrt{\frac{|\beta(bm+c)|}{(m+1)^3}}(x-ct)\right). \tag{5.13b}$$

The above solutions (5.12a, 5.13a) are called "solitary pattern solutions" by F. Xie and Z. Yan ([14]).

6. Conclusion

In summary, based on the previous exact solutions (see 4.3-5.2, 5.6, 5.12, 5.13) which have been given by other authors ([1–5,14,17]), we have obtained the exact traveling wave solutions (see 4.2, 5.3-5.5, 5.7-5.11) of the $D(m, n)$ system in different regions of the parametric space by applying the method of dynamical systems. Especially, we have finded the solitary cusp wave solutions (peakons or valleyons) (see 5.7-5.8). The paper is a summary of exact traveling wave solutions to the $D(m, n)$ system, that is, it classified by types of solutions. The traveling wave solutions include other authors' results (see 4.3-5.2, 5.6, 5.12, 5.13) and our own new results (see 4.2, 5.3-5.5, 5.7-5.11). Our results are given in different regions of the parametric space by applying the dynamical system method. Especially, we obtained the solitary cusp wave solutions (peakons or valleyons) (see 5.7 and 5.8).

References

[1] A. Biswas and H. Triki, *1-Soliton solution of the $D(m, n)$ equation with generalized evolution*, Applied Mathematics and Computation, 2011, 217, 8482–8488.

[2] P.F. Byrd and M.D. Fridman, *Handbook of elliptic integrals for engineers and scientists*, Berlin, Springer, 1971.

[3] A. Chen, D. Zhao and W. Huang, *Bifurcations of traveling wave solutions of Drinfel'd-Sokolov equtions*, Journal of Yunnan University (Natural Sciences Edition), 2007, 29(S1), 4–7.

[4] X. Deng, J. Cao and X. Li, *Travelling wave solutions for the nonlinear dispersion Drinfel'd-Sokolov ($D(m, n)$) system*, Communications in Nonlinear Science and Numerical Simulation, 2010, 15(2), 281–290.

[5] G. Ebadi, E.V. Krishnan, S. Johnson and A. Biswas, *Cnoidal wave, snoidal wave, and soliton solutions of the $D(m, n)$ equation*, Arabian Journal of Mathematics, 2013, (2), 19–31.

[6] M. Gurses and A. Karasu, *Integrable KdV systems: recursion operators of degree four*, Physics Letters A, 1999, 251(4), 247–249.

[7] J. Hu, *A new method of exact travelling wave solution for coupled nonlinear differentialequations*, Physics Letters A, 2004, 325(1), 37–42.

[8] J. Li, *Bifurcations and exact traveling wave solutions for a model of nonlinear pulse propagation in optical fibers*, International Journal of Bifurication and Chaos, 2014, 24(6), 1450088-1–15.

[9] J. Li, *Geometric properties and exact travelling wave solutions for the generalized Burger-Fisher equation and the Sharma-Tasso-Olver equation*, Journal of Nonlinear Modeling and Analysis, 2019, 1(1), 1–10.

[10] J. Li, *Singular nonlinear travelling wave equations: Bifurcations and Exact Solutions*, Science Press, Beijing, 2013.

[11] Y. Long, W. Rui, B. He and C. Chen, *Bifurcations of travelling wave solutions for generalized Drinfeld-Sokolov equations*, Applied Mathematics and Mechanics, 2006, 27(11), 1549–1555.

[12] X. Lu, L. Lu and A. Chen, *New peakons and periodic peakons of the modified Camassa-Holm equation*, Journal of Nonlinear Modeling and Analysis, 2020, 2(3), 345–353.

[13] Z. Wen and K. Zhao, *Qualitative analysis and periodic cusp waves to a class of generalized short pulse equations*, Journal of Nonlinear Modeling and Analysis, 2020, 2(4), 565–571.

[14] F. Xie and Z. Yan, *New exact solution profiles of the nonlinear dispersion Drinfel'd-Sokolov ($D(m,n)$) system*, Chaos, Solitons & Fractals, 2009, 39(2), 866–872.

[15] S. Xie, X. Hong and T. Jiang, *Planar bifurcation method of dynamical system for investigating different kinds of bounded travelling wave solutions of a generalized Camassa-Holm equation*, Journal of Applied Analysis and Computation, 2017, 7(1), 278–290.

[16] S. Xie, X. Hong and J. Lu, *The bifurcation travelling waves of a generalized Broer-Kaup equation*, Journal of Applied Analysis and Computation, 2020, Online First.

[17] K. Zhang, S. Tang and Z. Wang, *Bifurcations of travelling wave solutions for the nonlinear dispersion Drinfel'd-Sokolov ($D(m,n)$) system*, Applied Mathematics and Computation, 2010, 217(4), 1620–1631.